Review Article

Christian Freitag*, Leon Pauly, Daniel J. Förster, Margit Wiedenmann, Rudolf Weber, Taras V. Kononenko, Vitaly I. Konov and Thomas Graf

Residual heat generated during laser processing of CFRP with picosecond laser pulses

Abstract: One of the major reasons for the formation of a heat-affected zone during laser processing of carbon fiber-reinforced plastics (CFRP) with repetitive picosecond (ps) laser pulses is heat accumulation. A fraction of every laser pulse is left as what we termed residual heat in the material also after the completed ablation process and leads to a gradual temperature increase in the processed workpiece. If the time between two consecutive pulses is too short to allow for a sufficient cooling of the material in the interaction zone, the resulting temperature can finally exceed a critical temperature and lead to the formation of a heat-affected zone. This accumulation effect depends on the amount of energy per laser pulse that is left in the material as residual heat. Which fraction of the incident pulse energy is left as residual heat in the workpiece depends on the laser and process parameters, the material properties, and the geometry of the interaction zone, but the influence of the individual quantities at the present state of knowledge is not known precisely due to the lack of comprehensive theoretical models. With the present study, we, therefore, experimentally determined the amount of residual heat by means of calorimetry. We investigated the dependence of the residual heat on the fluence, the pulse overlap, and the depth of laser-generated grooves in CRFP. As expected, the residual heat was found to increase with increasing groove depth. This increase occurs due to an indirect heating of the kerf walls by the ablation plasma and the change in the absorbed laser fluence caused by the altered geometry of the generated structures.

Keywords: calorimetry; carbon fiber-reinforced plastics; CFRP; laser processing; residual heat.

1 Introduction

One major reason for the reduction of the quality of laser processes is the occurrence of heat-affected zones. When laser processing CFRP with unsuitable parameters, the formation of a matrix evaporation zone (MEZ) can be observed [1]. The matrix evaporation zone is the area next to the ablation zone where the polymer matrix evaporates while the carbon fibers remain. The formation of a MEZ is a consequence of the considerably different thermosphysical properties of the matrix and the fibers. The MEZ usually has its maximum extent in the direction along the carbon fibers [2–6]. The longitudinal thermal conductivity of the carbon fibers along their axis of symmetry is 10× higher than the one in transversal direction and about a factor of 200 higher than the one of the matrix material [7–9]. Additionally, the carbon fibers have a vaporization temperature of typically about 4000 K [10, 11] and a latent heat of 43,000 kJ/kg [12], while epoxy resins have a significantly smaller vaporization temperature of 800 K [10] and a considerably smaller latent heat of about 1000 kJ/kg [13].

A negligibly small extent of the MEZ (<1 μm) can be achieved by applying laser pulses with an intensity exceeding 10^9 W/cm^2 [14]. Such intensities are usually provided by lasers with pulse durations <100 ns. Virtually perfect quality was indeed demonstrated using such laser systems to process CFRP [15]. However, even when processing the material with sufficient high intensities, the extent of the MEZ can still vary in a wide range from no visible thermal damage [15] up to a few millimeters [16–20]. In this case, the formation of a MEZ is mainly caused by heat accumulation between subsequent laser pulses

*Corresponding author: Christian Freitag, Institut für Strahlwerkzeuge (IFSW), Universität Stuttgart, Pfaffenwaldring 43, 70569 Stuttgart, Germany, e-mail: christian.freitag@ifsw.uni-stuttgart.de
Leon Pauly, Daniel J. Förster, Margit Wiedenmann, Rudolf Weber and Thomas Graf: Institut für Strahlwerkzeuge (IFSW), Universität Stuttgart, Pfaffenwaldring 43, 70569 Stuttgart, Germany
Taras V. Kononenko and Vitaly I. Konov: Natural Sciences Center, General Physics Institute, Vavilov Str. 38, 119991 Moscow, Russia; and National Research Nuclear University "MEPhI", Kashirskoye shosse 31, 115409 Moscow, Russia

(HAP) and heat accumulation between subsequent scans (HAS) [21, 22].

Heat accumulation describes the effect of an increase in the temperature if the time between two subsequent heat inputs is too short for a complete cool down of the material back to its initial temperature [22]. A comprehensive analytical description of the temperature increase $\Delta T_{HA,nD}$ at the location of the heat deposition caused by heat accumulation is given by the so-called 'heat accumulation equation'

$$\Delta T_{HA,nD}\left(t=\frac{N_P}{f_P}\right)=\frac{Q_{nD}}{\rho \cdot c_p \sqrt{\left(\frac{4 \cdot \pi \cdot \kappa}{f_P}\right)^{nD}}}\sum_{N=1}^{N_P}\frac{1}{\sqrt{N^{nD}}} \qquad (1)$$

where Q_{nD} is the heat source in an infinitely short temporal δ-peak, N_P is the number of pulses, f_P is the pulse repetition rate, ρ is the mass density of the material, c_p is its specific heat capacity, $\kappa = \lambda_{th}/(\rho \cdot c_p)$ is the thermal diffusivity, λ_{th} is the heat conductivity, t is the time, and $nD \in [1, 2, 3]$ is the dimensionality of the heat flow; a detailed description of the heat accumulation equation and its variables can be found in Ref. [22]. When applying the heat accumulation Eq. (1), the most involved task is the exact specification of the heat source Q_{nD}, which depends on how much of the absorbed laser energy actually is left behind in the material as residual heat E_{res} after completion of the ablation induced by a single laser pulse.

2 Energy balance and the residual heat

The heat sources Q_{1D} = energy E_{res} per unit area, Q_{2D} = energy E_{res} per unit length, and Q_{3D} = energy E_{res} define the heat that is released in an infinitely short time at $t = 0$ [22]. All three heat sources have in common, that the energy E_{res}, which heats the material, is a fraction of the incident pulse energy E_P. This fraction is often referred to as residual heat [23] or residual thermal energy [24, 25]. For the following discussion, we express the relation between the incident pulse energy E_P, the absorbed energy $E_A = \eta_A \cdot E_P$, and the residual heat E_{res} by where η_A is the absorptance of the workpiece, $\eta_{resP} = \eta_{resA} \cdot \eta_A$ is the residual heat coefficient

$$E_{res} = \eta_{resP} \cdot E_P = \eta_{resA} \cdot \eta_A \cdot E_P = \eta_{resA} \cdot E_A \qquad (2)$$

relating E_{res} to the incident pulse energy E_P, and η_{resA} is the residual heat coefficient relating E_{res} to the absorbed energy E_A. For single-pulse ablation of metals, the
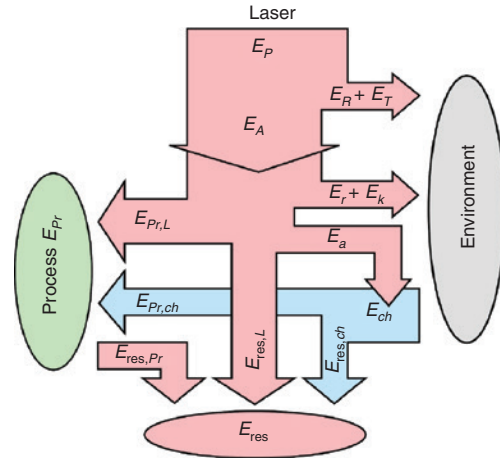

Figure 1: Energy balance associated to an ablation processes induced by one single laser pulse.

dependence of the residual energy coefficient on the laser fluence is reported in Refs. [23–25]. The influence of the ambient medium on the residual heat is reported in Refs. [24] and [25].

In order to unambiguously define the coefficients η_{resP} and η_{resA}, it is important to understand the influence of all effects contributing to the heating of the material, including potentially occurring chemical reactions with the ambient atmosphere. The complete energy balance associated to an ablation process induced by a single pulse with the incident energy E_P is schematically shown in Figure 1.

From the incident energy E_P, only the fraction $E_A = \eta_A \cdot E_P$ given by the aborptance η_A is absorbed by the workpiece. For the following, we assume that the absorbed energy is completely thermalized (hence, converted to heat). Radiation that is not absorbed is either reflected at the workpiece, amount E_R, and/or transmitted through the workpiece, amount E_T (e.g. when laser processing glass). These amounts of energy (E_R and E_T) are lost and cannot contribute to the intended laser process.

Also, part of the absorbed Energy E_A may be lost by the emission of thermal radiation, amount E_r, and convective cooling, amount E_k. The part $E_{Pr,L}$, however, directly contributes to the desired process and is, e.g. spent for heating, melting, evaporating, and removing the material during laser ablation. The other part $E_{res,L}$ of the absorbed energy does not contribute to the laser-induced process and is directly left in the material as residual heat. Finally, a further amount E_a of the absorbed energy may serve as activation energy to induce chemical reactions such as oxidation. When these chemical reactions are exothermal, the resulting reaction enthalpy H_R may be provided as an additional energy input. Together with the activation energy, this amounts to a total heat input of $E_{ch} = E_a + H_R$.

Again, one part $E_{Pr,ch}$ of this chemically produced energy may contribute to the desired process in the same way as $E_{Pr,L}$, while the other part $E_{res,ch}$ is left in the material and further increases the amount of residual heat.

In a first step, the process energy $E_{Pr} = E_{Pr,L} + E_{Pr,ch}$ is spent to perform the desired process (e.g. ablation) and, therefore, is removed from the workpiece. Some of this energy can, however, be transferred back into the work piece, e.g. due to heating of the kerf walls by the hot ablation plume or plasma during laser cutting. This constitutes a further contribution to the residual heat left in the workpiece and is termed $E_{res,Pr}$.

The total amount of residual heat after the completion of the processes induced by one single laser pulse is, therefore, given by

$$E_{res} = E_{res,L} + E_{res,ch} + E_{res,Pr}. \tag{3}$$

Considering the contributions by potentially occurring chemical reactions, the residual heat coefficients introduced above explicitly yield

$$\eta_{resP} = \frac{E_{res}}{E_P} = \frac{E_{res,L} + E_{res,ch} + E_{res,Pr}}{E_P}. \tag{4}$$

and

$$\eta_{resA} = \frac{E_{res}}{E_A} = \frac{E_{res,L} + E_{res,ch} + E_{res,Pr}}{E_A}. \tag{5}$$

Note that depending on the amount of the reaction enthalpy H_R, the two coefficients may even be larger than unity, which simply expresses the fact that, in this case, more than just the laser energy has contributed to the heating of the workpiece.

In the following, we would like to present the measurements of the residual heat coefficient when laser processing CFRP with a ps laser.

3 Experimental investigations

3.1 Experimental setup

A Lumentum Duetto laser system (Lumentum Switzerland AG, Schlieren, Zurich, Switzerland) was used for the experiments. This laser provides a beam with a wavelength of 1064 nm, a pulse repetition rate that can be varied between 50 kHz and 8.2 MHz, and a pulse duration of about 10 ps. Within the presented study, we kept the pulse repetition rate at a constant value of 50 kHz. The maximum average power available at this pulse frequency was 8.7 W. The beam quality was $M^2 \approx 1.06$. For the beam movement, we used a scanner system (SCANLAB AG, Puchheim, Germany) equipped with an f-Theta optics (Sill Optics GmbH & Co. KG, Wendelstein, Germany)

with a focal length of 80 mm. The radius of the resulting focal spot was measured to be 14.5 μm ($1/e^2$ intensity level). The polarization of the laser beam was linear and always oriented perpendicular to the axes of the carbon fibers.

The processed samples consisted of unidirectional CFRP made from HS150 EE24 REM Carbon UD Prepreg from SEAL S.p. A. The carbon fibers used within this prepreg material are T700 fibers from Toray Industries, Inc., and the matrix material is an REM epoxy resin. In view of the calorimetric experiments, the CFRP samples with sizes of 16×16 mm were polished down to a thickness of about 0.3–0.4 mm. As the thermal conductivity perpendicular to the carbon fibers and in the matrix material is small, we used such thin samples to ensure a quick and uniform heating of the samples. The top side of the sample was polished as well to remove the thick top matrix layer. The temperature of the samples was measured by means of a thermocouple Type K attached to the bottom of the samples. The thickness of the thermocouple wire was 0.5 mm. To compensate for local irregularities of the CFRP material, a thin copper plate with a thickness of 100 μm was positioned between the thermocouple and the samples. Heat paste was used to improve the thermal contact between the CFRP samples, copper plate, and thermocouple. The heating of the copper plate as well as the heat paste was taken into account during data evaluation. The samples were placed in a sample holder made of aluminum oxide with a minimum contact area to minimize losses by heat conduction into the holder. The sampling rate of the temperature measurement was 2.5 Hz.

3.2 Measurement methods

3.2.1 Calorimetry: The residual heat generated in the laser-processed samples was determined by means of calorimetry according to DIN EN ISO 11551. The samples were irradiated by the laser beam for a given irradiation time t_{irr}. As exemplarily shown in Figure 2, the temperature of the sample was measured during this irradiation as well as during the subsequent cooling phase with a
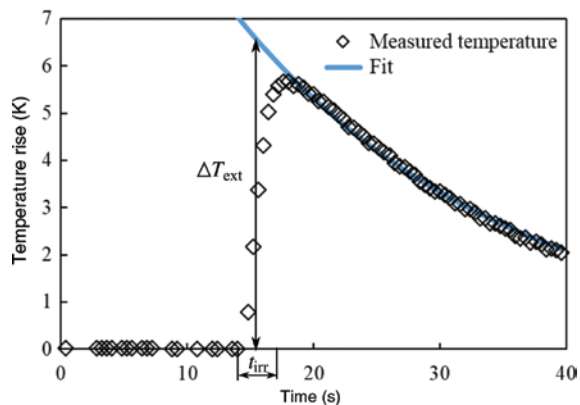

Figure 2: Temperature measurement of a CFRP sample irradiated by a laser beam with a fluence $\Phi_0 = 157$ J/cm², a pulse repetition rate of $f_p = 16.7$ kHz, a focal diameter $d_f = 29$ μm, a wavelength of $\lambda = 1064$ nm, a feed rate of $v_f = 2500$ mm/s, an irradiation time of $t_{irr} = 3$ s, and a linear polarization perpendicular to the carbon fibers. With these parameters, the individual pulses did not overlap on the sample.

duration of at least 200 s. Beginning from the maximum temperature rise, the function

$$T(t) = A_c + B_c \cdot e^{-\gamma_c \cdot t} \tag{6}$$

was fitted to the measured temperatures, where A_c, B_c, and γ_c are fitting parameters. The temperature increase ΔT_{ext} at the middle of the irradiation time t_{irr} then was extrapolated as indicated in Figure 2.

From the extrapolated temperature increase ΔT_{ext}, the residual energy coefficient η_{resP} can be calculated by

$$\eta_{resP} = f_c \cdot \frac{\Delta T_{ext} \cdot \sum_i m_i \cdot c_{p,i}}{E_{inc}} \tag{7}$$

where $E_{inc} = f_P \cdot t_{irr} \cdot E_P$ is the total laser energy incident on the sample, m_i is the mass of the heated components (CFRP sample, copper plate, and heat paste), $c_{p,i}$ are the specific heat capacities of the heated components, and f_c is a corrective factor for materials with low thermal conductivity. This corrective factor is necessary because the thermal conductivity of the carbon fibers perpendicular to their axis of symmetry and of the matrix material is low (see DIN EN ISO 11551). The corrective factor was measured to be $f_c = 1.126$ for our experiments. The specific heat capacity for the carbon fibers is $c_{p,CF} = 710$ J/kg·K [26], for the matrix material $c_{p,M} = 1960$ J/kg·K [27], for copper $c_{p,Cu} = 385$ J/kg·K, and for the heat paste, which consisted of 45% methylsilicone, 50% aluminum oxide, and 5% diamond, it was $c_{p,HP} = 1110$ J/kg·K. The mass of the heat paste was measured to be about $m_{HP} = 0.0038$ g, the mass of the copper plate was measured to be $m_{Cu} = 0.152$ g, and the mass of each CFRP sample was measured individually.

3.2.2 Absorptance: According to Eq. (2), the absorptance η_A must be known to determine the heat coefficient η_{resA} from the measured residual heat E_{res} and the known incident laser energy E_P. For normal incidence of the laser beam on a flat CFRP surface with a polarization that is orientated perpendicular to the carbon fibers, the absorptance was measured to be 94% [28]. The influence of a laser-generated ablation geometry on the absorptance was modeled following the basic considerations introduced by Gouffé [29]. Approximating the shape of the ablation front within the laser-generated grooves by a cone as shown in Figure 3A, where d_f is the focal diameter and s is

the groove depth, yields the absorptance values shown in Figure 3B. Although the geometry of the interaction zone deviates from the assumed cone as it is open toward the generated groove on the back side, it can, nevertheless, be concluded that the absorptance quickly converges to almost 100% already for an aspect ratio of >1. Because of the high absorptivity of 94% of the CFRP material, the possible uncertainty of the thus estimated absorptance anyway is limited to only a few percent.

4 Experimental results

4.1 Influence of the laser fluence on the residual heat coefficient

For a laser radiation incident on a flat CFRP surface, the heat coefficient η_{resA} as a function of the laser fluence is shown in Figure 4. For this measurement, the laser beam was moved over the workpiece with a scanner system at a high feed rate of 2.5 m/s to ensure that the individual pulses did not overlap on the sample (distance of 15 µm between the pulses). Hence, each laser pulse impinged on a non-processed area of the surface. The laser pulses were distributed evenly on the surface to obtain a homogeneous temperature of the workpiece. The pulse frequency was constant at 50 kHz. As seen from Figure 4, the highest residual heat coefficient of $\eta_{resA} = 64\%$ was found for the lowest fluence of $\Phi_0 = 0.32$ J/cm² used in our experiments, which is still above the ablation threshold. With increasing fluence, the residual heat coefficient decreases to about $\eta_{resA} = 25\%$ at a fluence of about $\Phi_0 = 52$ J/cm². For fluences $\Phi_0 \leq \Phi_{th} \approx 0.2$ J/cm², with Φ_{th} being the threshold fluence, the complete absorbed pulse energy is transferred into heat, which means that $\eta_{resA} = 100\%$.
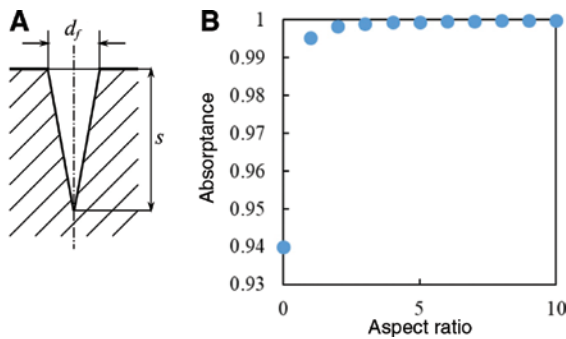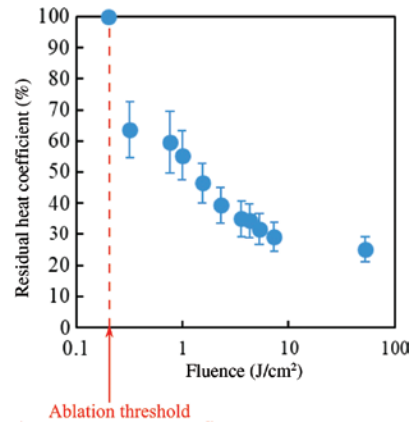
Figure 3: Influence of a laser-generated geometry on the absorptance. (A) Geometry chosen to model the increased absorption of radiation within grooves [29]. (B) Absorptance as a function of the aspect ratio s/d_f of the model geometry. For a flat surface, the absorptance of radiation with a linear polarization oriented perpendicular to the carbon fibers is 94% [28].

Figure 4: Residual heat coefficient η_{resA} for laser pulses incident on a flat CFRP surface as a function of the fluence. The wavelength of the laser radiation was 1064 nm, the pulse duration 10 ps, and the polarization was oriented perpendicular to the carbon fibers.

For the situation considered here with separated laser pulses irradiating a flat surface at normal incidence, it can be assumed that the amount of indirectly reintroduced heat $E_{res,Pr}$, originating from, e.g. hot ablation products or a plasma plume is small as the ablated material can freely expand into the half space above the workpiece. Therefore, the amount of residual heat is mainly governed by the amount of energy $E_{res,L}$ that is immediately transferred into residual heat. Especially at the lower fluences, the influence the chemically introduced energy $E_{res,ch}$ due to oxidation might become noticeable [2], but the distinction of this contribution was beyond the scope of the present study and will be subject of future investigations.

4.2 Influence of a pulse overlap

Increasing the pulse overlap by decreasing the feed rate leads to the generation of a groove and increases the effect of heat accumulation. As a measure of the pulse overlap, we calculated the number of pulses per spot according to $N_P = d_f f_p / v_f$. The depth of the generated grooves as a function of the pulse overlap is shown in Figure 5 by the orange diamonds together with the measured residual heat coefficient η_{resA} shown by the blue circles. The fluence was kept constant at a value of 52 J/cm², and the pulse repetition rate was 50 kHz. Without any pulse overlap, the same residual heat coefficient of $\eta_{resA} = 25\%$ is already presented in Figure 4. An increase in the number of pulses per spot to $N_P = 10$ and $N_P = 20$ leads to a slight decrease
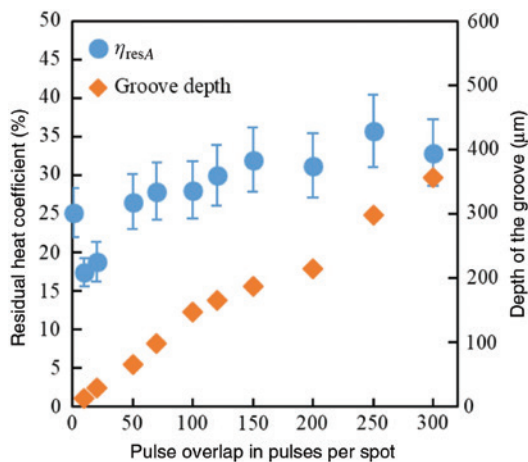
in the residual heat coefficient to about $\eta_{resA,10} = 17\%$ and $\eta_{resA,20} = 19\%$, respectively. Possible reasons are a more efficient material removal due to the preheating of the material by the previous laser pulses or a cooling of the whole material due to vaporizing matrix material. When more material is removed, less excessive energy is potentially deposited as residual heat in the material. When a MEZ is generated, energy that is spent on the vaporization of the matrix material does not remain in the material as heat. As can be seen from Figure 6A, already for 20 pulses per spot, a MEZ with an extent of about 100 µm is generated. The extent of the MEZ grows with increasing number of pulses per spot (see Figure 6B and C). Further investigations will be required to verify these interpretations.

With a further increasing number of pulses per spot, the residual heat coefficient increases as well. Within the range of parameters that were investigated, a stable level of the residual heat coefficient at a value of about $\eta_{resA} = 32\%$ is reached for a number of pulses $N_P \geq 150$. One possible explanation for the increased residual heat coefficient may be the decrease in the effective laser fluence at the irradiated kerf wall with increasing groove depth. According to Figure 4, a decrease in the laser fluence results in an increase in the heat coefficient. As soon as the fluence within the groove is below the ablation threshold, all absorbed energy will be converted into heat. In this case, the residual heat coefficient should be close to 100%. Another possible reason is re-deposition of energy as described in section 2: With increasing groove depth, the expanding ablation products and plasma can interact with the groove walls over a larger area reintroducing
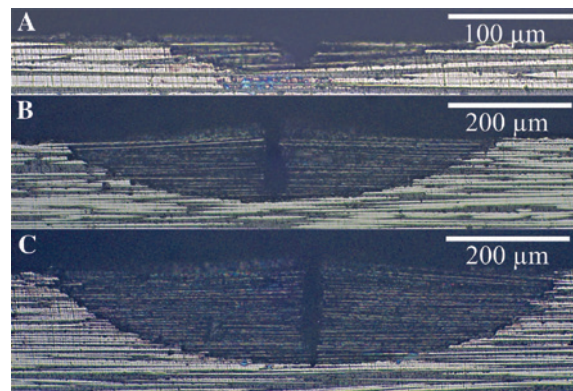
Figure 5: Residual heat coefficient η_{resA} and depth of the generated grooves as a function of the pulse overlap. The applied fluence was 52 J/cm², the pulse repetition rate was 50 kHz, the wavelength was 1064 nm, the pulse duration was 10 ps, and the polarization was oriented perpendicular to the carbon fibers.

Figure 6: Cross sections of the grooves generated with a different number of pulses per spot: (A) 20 pulses per spot, (B) 100 pulses per spot, (C) 150 pulses per spot. The applied fluence was 52 J/cm², the pulse repetition rate was 50 kHz, the wavelength was 1064 nm, the pulse duration was 10 ps, and the polarization was oriented perpendicular to the carbon fibers.
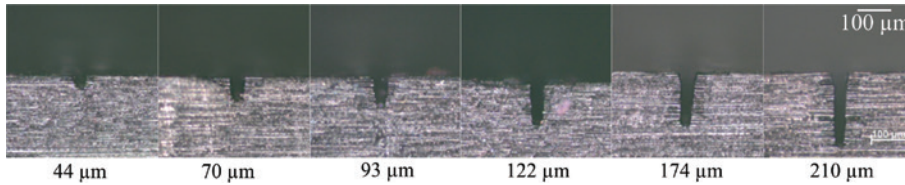
Figure 7: Cross sections of laser-generated grooves with different depths in CFRP. The applied fluence was 52 J/cm², the pulse repetition rate was 50 kHz, the wavelength was 1064 nm, the pulse duration was 10 ps, the feed rate was 300 mm/s, and the polarization was oriented perpendicular to the carbon fibers. To achieve higher groove depths, the number of scans was increased.

heat into the material. This re-deposited heat leads to an increase in the residual heat.

4.3 Influence of the depth of the groove

In order to isolate the influence of the groove depth from other related changes in the process such as heat accumulation, we applied the following procedure: in the first step, several grooves were generated with different depths, as shown in Figure 7. After the material cooled back down to room temperature, the residual heat coefficient was measured by coupling laser pulses into the geometry using a high feed rate of 2 m/s, which leads to a spatial separation of the individual pulses (distance of 5 µm between the pulses). Again, the nominal incident fluence was constant at 52 J/cm², and the pulse frequency was 50 kHz.

The results are shown in Figure 8. The data point at a groove depth of 0 µm is the same as in Figure 4 for the corresponding fluence. It can be seen from Figure 8 that with increasing groove depth, the heat coefficient increases until a maximum is reached. The residual heat coefficient stays constant at about $\eta_{resA} = 53\%$ for groove depths $d_{groove} \geq 70$ µm.

Again, the possible reasons for the increase in the residual heat coefficient η_{resA} with increasing groove depth are a decrease in the effective laser fluence due to the groove geometry and indirect heating of the material by expanding ablation products and plasma. Note that the values determined here are almost a factor of two higher than the ones shown in Figure 5. The residual heat coefficient for a groove depth of, e.g. 210 µm was found to be $\eta_{resA} = 53\%$ without any pulse overlap (Figure 8) but amounted to only $\eta_{resA} = 31\%$ for a similarly deep grove (214 µm) when the number of pulses per spot is 200 (Figure 5). This, again, suggests the assumption that either the heat accumulation effect associated with the high number of pulses in the latter case leads to an enhanced removal of hot material that is preheated by the series of pulses and, therefore, reducing the heat left in the workpiece or cooling of the whole material occurs due to vaporizing matrix material.

5 Conclusion

In summary, we have reported on calorimetric determination of the residual heat coefficient for laser processing of CFRP with ultra-short pulses at a wavelength of 1064 nm and a pulse duration of 10 ps. For spatially separated laser pulses, it was found that the residual heat coefficient decreases with increasing laser fluence. When increasing the pulse overlap, the residual heat coefficient was measured to first decrease ($N_p = 10$ to 20) and then increase to beyond the values obtained without pulse overlap ($\eta_{resA} = 32\%$ with pulse overlap compared to $\eta_{resA} = 25\%$ for spatially separated pulses). To isolate the influence that the generated groove geometry has on the residual heat, spatially separated pulses were irradiated into pre-processed grooves. The result here was a larger residual heat coefficient compared to the value measured with pulse
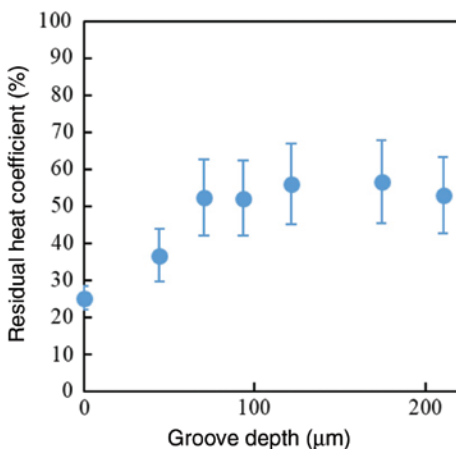

Figure 8: Influence of the groove depth on the residual heat coefficient η_{resA}. Spatially separated laser pulses were coupled into the grooves. The applied fluence was 52 J/cm², the pulse repetition was 50 kHz, the wavelength was 1064 nm, the pulse duration was 10 ps, and the polarization was oriented perpendicular to the carbon fibers.

overlap during the processing of the groove ($\eta_{resA} = 53\%$ without pulse overlap compared to $\eta_{resA} = 32\%$ with pulse overlap for grooves of similar depth). Overall, mainly two effects can explain the influence of the geometry on the residual heat: First, the laser fluence is effectively reduced within the groove as the energy is distributed on a larger area, which, on its turn, already was found to lead to an increased residual heat. Second, the re-deposition of heat by the expanding ablation products that interact with the walls of the groove becomes more relevant with increasing groove depth. The presented experiments are a first approach toward a better understanding of the physical processes that determine the residual heat during laser processing of CFRP. Further research especially also on the influence of chemically released energy and the reintroduced heat, e.g. by hot ablation products is needed for a more detailed description of the residual heat coefficient. This investigation will also have to be extended to other processed materials and other laser processes such as drilling or multiple-scan cutting.

References

[1] C. Freitag, V. Onuseit, R. Weber and T. Graf, Phys. Procedia 39, 171 (2012).

[2] T. V. Kononenko, C. Freitag, M. S. Komlenok, V. Onuseit, R. Weber, et al., J. Appl. Phys. 115, 103107 (2014).

[3] C. T. Pan and H. Hocheng, J. Mater. Process. Technol. 62, 54 (1996).

[4] C. T. Pan and H. Hocheng, J. Mater. Eng. Perform. 7, 751 (1998).

[5] E. Uhlmann, G. Spur, H. Hocheng, H. S. Liebelt and C. T. Pan, Int. J. Mach. Tool. Manuf. 39, 639 (1999).

[6] C. T. Pan and H. Hocheng, Compos. Part A Appl. Sci. Manuf. 32, 1657 (2001).

[7] C. Pradere, J. C. Batsale, J. M. Goyhénèche, R. Pailler and S. Dilhaire, Carbon 47, 737 (2009).

[8] S. D. McIvor, M. I. Darby, G. H. Wostenholm, B. Yates, L. Banfield, et al., J. Mater. Sci. 25, 3127 (1990).

[9] R. Rolfes and U. Hammerschmidt, Compos. Sci. Technol. 54, 45 (1995).

[10] P. Sheng and G. Chryssolouris, J. Compos. Mater. 29, 96 (1995).

[11] Y. Zhang, J. R. G. Evans and S. Yang, J. Chem. Eng. Data 56, 328 (2011).

[12] G. Herzberg, K. F. Herzfeld and E. Teller, J. Phys. Chem.-US 41, 325 (1937).

[13] C. A. Griffs, R. A. Masumura and C. I. Chang, J. Compos. Mater. 15, 427 (1981).

[14] R. Weber, M. Hafner, A. Michalowksi and T. Graf, Phys. Procedia 12, 302 (2011).

[15] C. Freitag, M. Wiedenmann, J.-P. Negel, A. Loescher, V. Onuseit, et al., Appl. Phys. A Mater. 119, 1237 (2015).

[16] A. Wolynski, H. Haloui, P. Mucha, A. Gleiter, P. French, et al., in 'Proceedings of International Congress on Applications of Lasers & Electro-Optics ICALEO 2010', (Anaheim, USA, 26 September–30 September 2010).

[17] A. Wolynski, T. Herrmann, P. Mucha, H. Haloui and J. L'huillier, Phys. Procedia 12B, 292 (2011).

[18] R. Weber, C. Freitag, T. V. Kononenko, M. Hafner, V. Onuseit, et al., Phys. Procedia 39, 137 (2012).

[19] T. Herrmann, M. Stolze and J. L'huillier, Proc. SPIE 8972, 89721K (2014).

[20] M. Fujita, H. Ohkawa, M. Otsuka, T. Somekawa, Y. Maeda, et al., in 'Proceedings of International Congress on Applications of Lasers & Electro-Optics ICALEO 2014', (San Diego, USA, 19 October–23 October 2014).

[21] T. V. Kononenko, C. Freitag, M. S. Komlenok, V. Onuseit, R. Weber, et al., J. Appl. Phys. 118, 103105 (2015).

[22] R. Weber, T. Graf, P. Berger, V. Onuseit, M. Wiedenmann, et al., Opt. Express 22, 11312 (2014).

[23] F. Bauer, A. Michalowski and S. Nolte, J. Laser Micro Nanoen. 10, 325 (2015).

[24] A. Y. Vorobyev and C. Guo, Opt. Express 14, 13113 (2006).

[25] A. Y. Vorobyev, V. M. Kuzmichev, N. G. Kokody, P. Kohns, J. Dai, et al., Appl. Phys. A 82, 357 (2006).

[26] B. Sundqvist, O. Sandberg and G. Bäckström, J. Phys. D Appl. Phys. 10, 1397 (1977).

[27] B. T. Kelly, in 'Physics of Graphite', (Applied Science Publishers, London and New Jersey, 1981).

[28] C. Freitag, L. Alter, R. Weber and T. Graf, in 'Proc. of Lasers in Manufacturing 2015', (München, Germany, 2015).

[29] A. Gouffé, Revue d'Optique 24, 1 (1945).